Recruitment of CD11b$^+$Ly6C$^+$ monocytes in non-small cell lung cancer xenografts challenged by anti-VEGF antibody

XIE-WAN CHEN[1,2], JIAN-GUO SUN[2], LU-PING ZHANG[2], XING-YUN LIAO[2] and RONG-XIA LIAO[1]

[1]Medical English Department, College of Basic Medicine, Third Military Medical University, Chongqing 400038; [2]Cancer Institute of People's Liberation Army, Xinqiao Hospital, Third Military Medical University, Chongqing 400037, P.R. China

Received September 17, 2015; Accepted March 3, 2017

DOI: 10.3892/ol.2017.6236

Abstract. A series of antibodies against vascular endothelial growth factor (VEGF) have been developed for the treatment of various types of cancer, including non-small cell lung cancer (NSCLC) in recent years. However, tumors frequently demonstrate resistance to these strategies of VEGF inhibition. Efforts to better understand the mechanism underlying the acquired resistance to anti-VEGF antibodies are warranted. In the present study, in order to develop a xenograft model of acquired resistance to anti-VEGF antibody, xenografts of human adenocarcinoma A549 cells were generated through the successive inoculation of tumor tissue explants into first (F1), second (F2) and third (F3) generations of mice treated with the anti-VEGF antibody B20. Tumor growth rate and vessel-forming ability, assessed via cluster of differentiation (CD) 31 staining, were significantly lower in the F1, F2 and F3 groups compared with in the F0 control group ($P<0.01$), suggesting that drug resistance was not successfully acquired. The percentages of CD11b$^+$ myeloid-derived suppressor cells and lymphocyte antigen 6C (Ly6C)$^+$ subsets were significantly smaller in F1, F2 and F3 groups compared with in F0 ($P<0.01$). However, the ratio of Ly6C$^+$ to CD11b$^+$ cells was significantly higher in the F3 group compared with in F0 and F1 groups ($P<0.01$), indicating increasing recruitment of the Ly6C$^+$ subset with successive challenges with the anti-VEGF antibody. In conclusion, the recruitment of CD11b$^+$Ly6C$^+$ monocytes increased with successive generations of NSCLC-xenografted mice challenged by B20, an anti-VEGF agent.

Correspondence to: Professor Rong-Xia Liao, Medical English Department, College of Basic Medicine, Third Military Medical University, 30 Gaotanyan Center Street, Shapingba, Chongqing 400038, P.R. China
E-mail: liaorx@aliyun.com

Professor Jian-Guo Sun, Cancer Institute of People's Liberation Army, Xinqiao Hospital, Third Military Medical University, Xinqiao Center Street, Shapingba, Chongqing 400037, P.R. China
E-mail: sunjg09@aliyun.com

Abbreviations: NSCLC, non-small cell lung cancer; VEGF, vascular endothelial growth factor; VEGFR, vascular endothelial growth factor receptor; MDSC, myeloid-derived suppressor cell; CD, cluster of differentiation; TAM, tumor-associated macrophage

Key words: angiogenesis, anti-vascular endothelial growth factor treatment, CD11b, Ly6C, non-small cell lung cancer

Introduction

Cancer is one of the leading causes of mortality worldwide, and lung cancer is one of the leading causes of cancer-associated mortality with a 5-year survival rate of ~16% (1). Representing >85% of lung cancer cases, non-small cell lung cancer (NSCLC) is the most common type (2). Of patients with NSCLC, >2/3 are initially diagnosed at an advanced stage, at which point palliative chemotherapy is the primary option. Although 30-40% of patients may respond to cytotoxic chemotherapy, the majority eventually suffer from disease progression (3). The survival rate of patients with advanced lung adenocarcinoma improved in the early 2000's, most probably due to the emergence of inhibitors of epidermal growth factor receptor, anaplastic lymphoma kinase and vascular endothelial growth factor (VEGF) (4).

Angiogenesis, a process mainly mediated by VEGF, has been demonstrated to be crucial for tumor growth, invasion and metastasis (5); although small tumors are able to obtain nutrients and oxygen through diffusion, the formation of new vasculature is critical for tumor expansion and metastasis (6). The associations between various measures of tumor aggressiveness and increases in intratumoral microvessel density illustrate the essential role of angiogenesis in tumor growth and metastasis (7).

The role of VEGF in angiogenesis has been well established (8-10). A range of evidence has suggested that VEGF and its receptors exhibit altered activity in various human cancer types (11). In general terms, VEGF expression correlates negatively with clinical outcome (12-14).

In 1971, it was proposed by Judah Folkman (15) that inhibiting angiogenesis may be an effective approach to anticancer therapy. More than 30 years after this original hypothesis, the first proof of anti-angiogenic therapy in NSCLC came with the approval of bevacizumab, a monoclonal antibody directed against human VEGF (16). Since then, a series of antibody-based agents against VEGF have been developed, the majority of which are undergoing clinical trials (16,17), including trials of patients with NSCLC (18). Despite promising clinical effects, resistance to these agents has been reported (19). Investigations into the

mechanisms underlying resistance to anti-VEGF antibodies are warranted in order for the successful advancement of these promising therapeutic agents.

Myeloid-derived suppressor cells (MDSCs) are a group of myeloid cells comprising precursors of macrophages, granulocytes, dendritic cells and myeloid cells at earlier stages of differentiation (20-23). In mice, these cells are broadly defined by their dual expression of Gr-1 and cluster of differentiation (CD) 11b. Evidence has demonstrated that tumor-infiltrating MDSCs are present in the peripheral blood of patients with different types of cancer, including lung, breast, and head and neck cancer (24,25). These MDSCs have been suggested to contribute to the development of resistance to several forms of treatment, including anti-angiogenic agents that target VEGF receptor (VEGFR) signaling (26-32).

The myeloid differentiation antigen Gr-1 consists of two epitopes, recognized by anti-lymphocyte antigen (Ly) 6G and anti-Ly6C antibodies, which divide $CD11b^+Gr\text{-}1^+$ MDSCs into $Ly6G^+$ granulocytes and $Ly6C^+$ monocytes (33). These two subpopulations may have different functions in infectious diseases and cancer (34-36). $Ly6C^{hi}$ monocytes have been reported to function as transient accessory cells to enhance angiogenesis and remodeling of existing small vessels into larger conduits upon their onsite 'education' by VEGF (37). There are two well-established polarized phenotypes of tumor-associated macrophages (TAMs): Classically activated macrophages (M1) and alternatively activated macrophages (M2) (38,39). It is generally accepted that M2 macrophages function in the moderation of inflammatory responses, promoting angiogenesis and contributing to tissue remodeling, all of which have been suggested to promote tumor progression (40-42). $Ly6C^{hi}$ inflammatory monocytes can also differentiate into M2 macrophages in autoimmune encephalomyelitis (43) or promote M2 macrophage polarization in acute tissue injury (44).

To better understand the mechanisms underlying resistance to anti-VEGF antibodies, an ideal model of anti-VEGF is required. The current study aimed to develop a model of acquired resistance to B20, a monoclonal antibody against VEGF, in nude mice following chronic exposure to B20. Subsequently, the migration of $CD11b^+Ly6C^+$ monocytes into the tumor tissue was detected. These investigations may provide the basis for strategies to improve the efficacy of anti-VEGF antibody treatments.

Materials and methods

Preparation of monoclonal antibody B20. The monoclonal antibody B20 is the mouse equivalent of bevacizumab (Avastin®), which is able to bind to mouse and human VEGF (45). B20 antibody was obtained from Genentech, Inc. (San Francisco, CA, USA) and administered intraperitoneally (150 mg/mouse) every 3 days.

Cell culture and reagents. The human NSCLC cell line A549 was purchased from the American Type Culture Collection (Manassas, VA, USA) and cultured in Dulbecco's modified Eagle's medium (DMEM) supplemented with 10% heat-inactivated fetal bovine serum, 4 mol/l glutamine, 50 U/ml penicillin and 50 mg/ml streptomycin. The cell line was cultured at 37˚C in 5% CO_2.

Xenotransplantation experiments. A total of 15 female BALB/c nude mice (age, 4-5 weeks; weight, 200-220 g) were purchased from the Experimental Animal Center of the Third Military Medical University (Chongqing, China). They were housed in a laminar flow room with specific pathogen-free conditions at a temperature of 22±2˚C and <40% humidity, with free access to food and water. A549 cells in the exponential growth stage were trypsinized, washed twice with serum-free DMEM and suspended in PBS. The cells ($2x10^6$/0.1 ml) were mixed with 0.1 ml of Matrigel (BD Biosciences, Franklin Lakes, NJ, USA) and injected subcutaneously into the lower right flank of the nude mice, establishing a tumor xenograft model. Tumor growth was monitored and measured with a vernier caliper, and tumor volume (V) was calculated based on the formula previously described (46):

$$V = \frac{\text{length x (width}^2)}{2}$$

Mice inoculated with A549 cells alone were used as the F0 control group (n=6). The F1 group (n=3) was injected with A549 cells and treated with B20 twice per week; tumor volume was monitored over time, and the mice were sacrificed on day 29 post-inoculation. Thereafter, the tumor explants were harvested from the F1 group, cut into fragments of 2-3 mm in diameter and transplanted into mice in the F2 generation (n=3), with B20 administered as for the F1 mice. Tumor volumes in the F2 mice were observed, and the mice were sacrificed on day 21 post-inoculation. Tumor explants from the previous generation were similarly inserted into F3 (n=3) mice, with B20 administered, and then F4 mice (n=3), without B20 treatment. Thereby, a total of five groups of mice were used in the present study, with each group composed of 3-6 animals. Following sacrifice of the mice, the volumes of the tumors were observed in the five groups and the growth curves were drawn. All animal procedures were conducted with the approval of the Ethical Committee of Third Military Medical University.

Immunofluorescence microscopy. For immunofluorescence analysis, tumor tissue was embedded in paraffin and cut into slices of 7-μm thickness for immunostaining using a Leica RM 2125 rotary microtome (Leica Microsystems, Inc., Buffalo Grove, IL, USA). The sections were dewaxed at 60˚C, serially immersed in solutions of decreasing alcohol concentration and subsequently boiled in 10 mM sodium citrate (pH 6.2) for 30 min for antigen retrieval. The tissue was then incubated in 3% hydrogen peroxide for 5 min, blocked with 1% bovine serum albumin and 5% goat serum (both Gibco; Thermo Fisher Scientific, Inc., Waltham, MA, USA) at room temperature for 1 h. Following 3 washes in cold PBS, the tissue was incubated overnight at 4˚C with primary antibody, followed by incubation with a secondary antibody at room temperature for 2 h. The nuclei were stained with DAPI solution (1:1,000; Sigma-Aldrich; Merck KGaA, Darmstadt, Germany). The primary antibodies used in the present study included anti-mouse antibodies directed against CD31 (cat. no., sc-376764), CD11b (cat. no., sc-20050) and Ly6C (cat. no., sc-271811; all 1:300 dilution; Santa Cruz Biotechnology, Inc., Dallas, TX, USA). DyLight 594 AffiniPure goat

Table I. CD31 and CD11b ratios in non-small cell lung cancer xenografts.

Group	CD31 ratio	CD11b ratio
F0	0.18±0.01[a]	0.16±0.02[a]
F1	0.11±0.01	0.10±0.01
F2	0.07±0.02	0.09±0.03
F3	0.05±0.01	0.06±0.01
F4	0.16±0.02[a]	0.15±0.03[a]

[a]P<0.01 vs. F1, F2 and F3 groups. All data are presented as the mean ± standard deviation. CD, cluster of differentiation; F0, mice injected with A549 cells only; F1, mice injected with A549 cells and treated with B20 twice weekly; F2, mice transplanted with F1 tumor explant and treated with B20 twice weekly; F3, mice transplanted with F2 tumor explant and treated with B20 twice weekly; F4, mice transplanted with F3 tumor explant with no treatment.

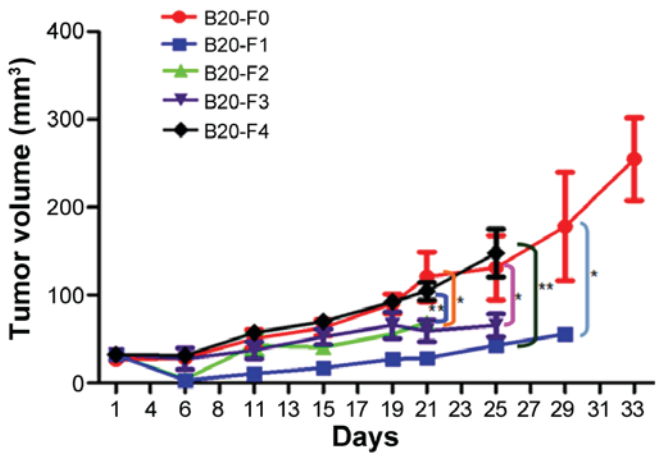

Figure 1. Tumor growth curves of non-small cell lung cancer xenografts. In the F1-F3 groups, the tumor sizes were similar, indicating the continuous inhibitory effects of anti-VEGF antibody on tumor growth. The tumor growth rate was significantly lower in the F3 group compared with in the F0 (control) group (P<0.01), suggesting that resistance to the B20 antibody was not successfully acquired. The tumor growth rate in the F4 group was similar to that in F0, indicating the withdrawal of inhibition by the anti-VEGF antibody. *P<0.01, F0 vs. F1/F2/F3; **P<0.05, F4 vs. F1/F2; n=3-6. VEGF, vascular endothelial growth factor; F0, mice injected with A549 cells only; F1, mice injected with A549 cells and treated with B20 twice weekly; F2, mice transplanted with F1 tumor explant and treated with B20 twice weekly; F3, mice transplanted with F2 tumor explant and treated with B20 twice weekly; F4, mice transplanted with F3 tumor explant with no treatment.

anti-mouse IgG (cat. no., A23410) and DyLight 488 AffiniPure goat anti-mouse IgG (cat. no., A23210; both 1:1,000 dilution; Abbkine Scientific Co., Ltd., Wuhan, China) were used as secondary antibodies. Immunofluorescence images were captured using a Nikon TE-2000E laser confocal microscope (magnification, x200, x400; Nikon Corporation, Tokyo, Japan). For analysis, images at x200 magnification of non-necrotic and viable tumor regions were obtained. At least 4 sections per tumor and 3 animals per group were analyzed. Image-Pro Plus software (MediaCybernetics, Inc., Rockville, MD, USA) was used to determine area densities or co-localization, as described previously (47).

Statistical analysis. The statistical significance of each set of experimental results was assessed using an analysis of variance or a Student's t-test. All statistical analyses were performed using SPSS v17.0 (SPSS Inc., Chicago, IL, USA). All data are presented as the mean ± standard deviation. P<0.05 was considered to indicate a statistically significant difference.

Results

Tumor growth curves. To determine whether resistance to the anti-VEGF antibody was acquired in a xenograft model, A549 cells were injected into the mice and the antibody administered generation by generation. Tumor growth curves were produced for each group and the tumor growth rates between different groups were compared (Fig. 1). At the endpoint of observation (day 21), the tumor volume was significantly larger in the F0 group compared with in F1, F2, and F3 groups (all P<0.01), suggesting continuous inhibition of tumor growth by the anti-VEGF B20 antibody. Although the antibody reduced the growth of xenograft tumors, the tumors grew progressively in F1, F2 and F3 groups during the course of the experiment; complete inhibition of tumor growth was not observed. In the F4 group, the tumor volume was significantly larger compared with that in the F1 and F2 groups (P<0.05), and was almost the same as in F0, reflecting the removal of anti-VEGF antibody-mediated inhibition. Overall, these findings indicated that the NSCLC xenograft model of acquired resistance to anti-VEGF antibody had not been successfully established.

Detection of CD31 staining. The ratio of endothelial cells (CD31-positive, red) to all cells in the field of vision (DAPI-positive, blue) was calculated to evaluate the vessel density and degree of angiogenesis. Immunostaining revealed that CD31 expression was higher in the F0 (control) and F4 groups compared with that in the F1-F3 groups (Fig. 2). CD31 expression progressively reduced from F1 (Fig. 2B) to F2 (Fig. 2C) to F3 (Fig. 2D), indicating the decreasing degree of angiogenesis and the inhibitory effects of the anti-VEGF antibody. The ratio of CD31/nucleus continuously decreased from the F1 to F2 to F3 groups, and was significantly lower in each of these three groups compared with in the F0 and F4 groups (all P<0.01; Table I). These results suggested that the B20 anti-VEGF antibody effectively inhibited blood vessel formation in the F1, F2 and F3 groups. Withdrawal of the drug from F4 group partially reversed the suppression of angiogenesis, but the lower vessel density in the F3 group compared with that in the F0 control indicated unsuccessful establishment of the anti-VEGF resistance model.

Assessment of the migration of CD11b$^+$ myeloid cells. The ratio of CD11b$^+$ myeloid cells (green) to cells in the field of vision (blue) was calculated. The blood vessels were simultaneously marked by CD31. Confocal microscopy demonstrated that the number of CD11b$^+$ myeloid cells was markedly higher in the F0 (control) and F4 groups compared with in the other groups (Fig. 3), and continuously decreased from F1 (Fig. 3B) to F2 (Fig. 3C) to F3 (Fig. 3D), suggesting the inhibition of MDSC migration by the anti-VEGF antibody. The ratio of CD11b/nucleus (CD11b ratio) progressively reduced from the F1 to F2 to F3 groups, and the CD11b ratio

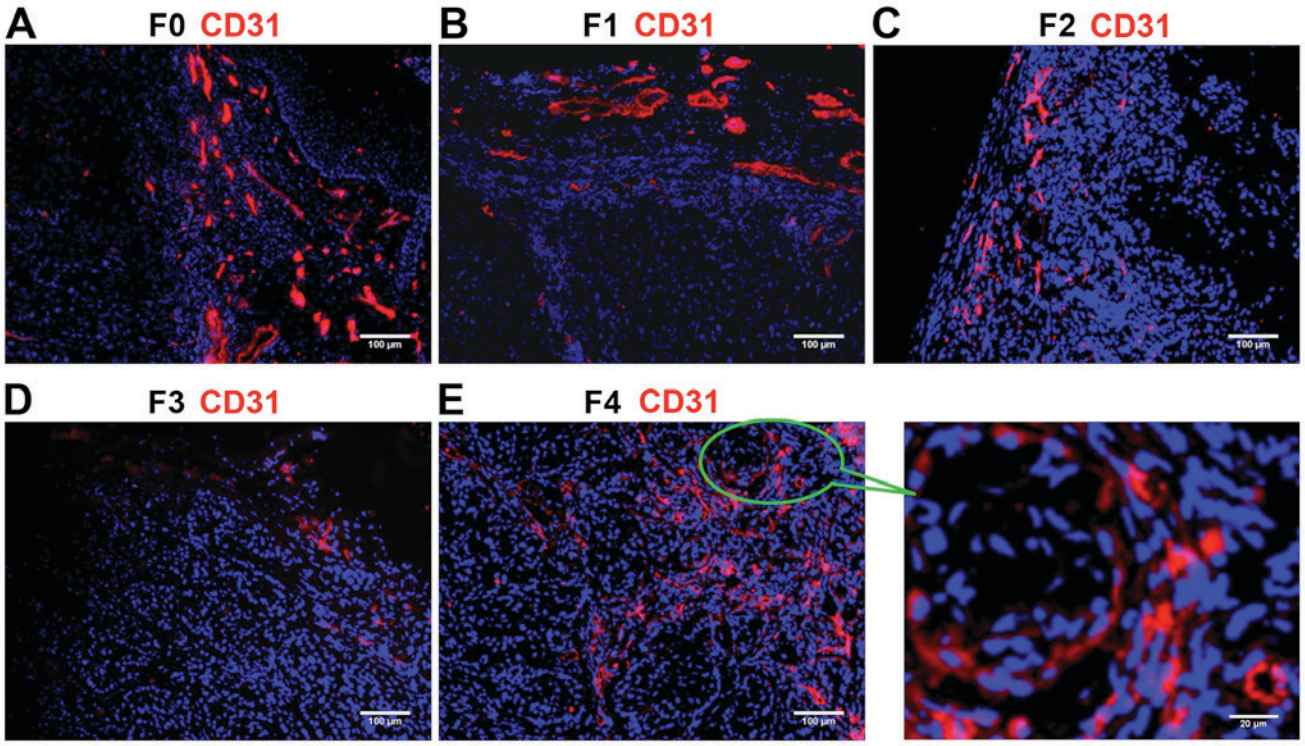

Figure 2. Immunostaining of CD31 (red) in non-small cell lung cancer xenografts. Blue fluorescence indicates DAPI (nuclear) staining. (A) The F0 (control) group exhibited high vessel density. (B) F1, (C) F2 and (D) F3 groups exhibited lower expression of CD31 compared with that in the F0 group. (E) The F4 group demonstrated similar vessel density to that in F0, and higher expression of CD31 compared with that in F1, F2 and F3. CD31, cluster of differentiation 31; F0, mice injected with A549 cells only; F1, mice injected with A549 cells and treated with B20 twice weekly; F2, mice transplanted with F1 tumor explant and treated with B20 twice weekly; F3, mice transplanted with F2 tumor explant and treated with B20 twice weekly; F4, mice transplanted with F3 tumor explant with no treatment.

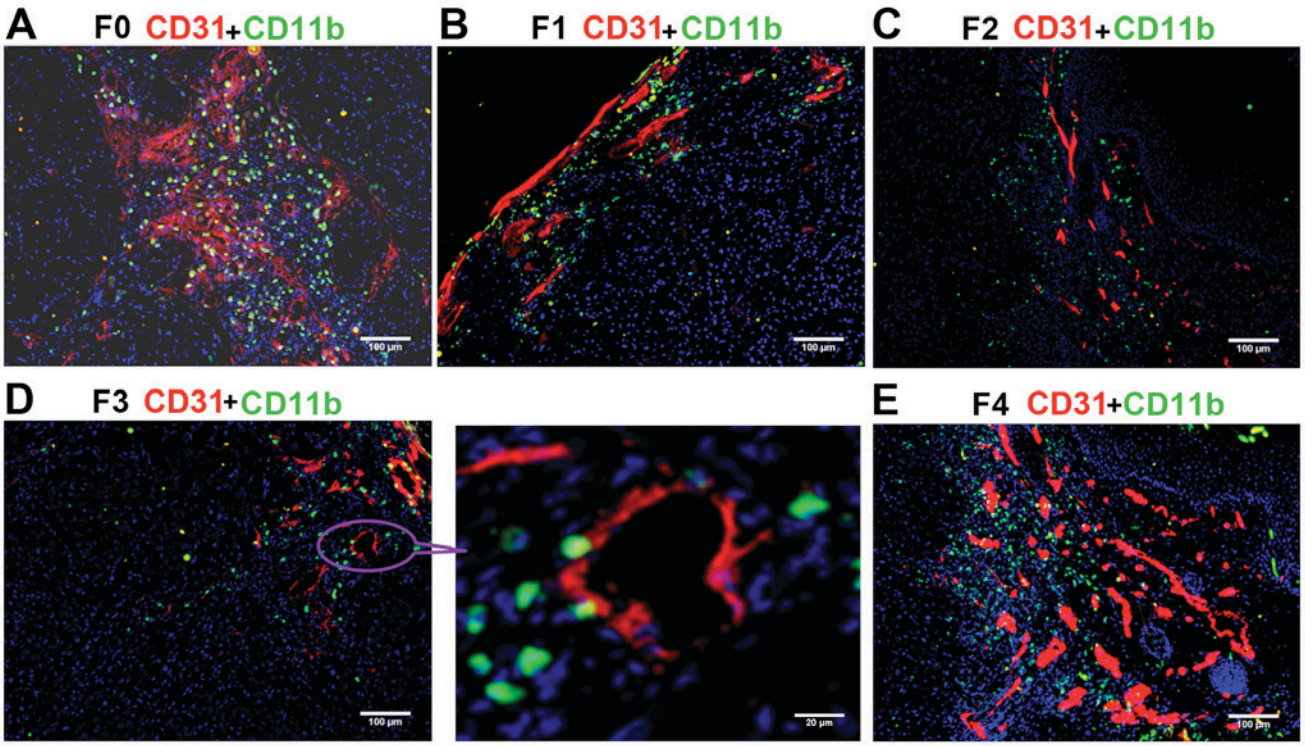

Figure 3. Immunostaining of CD11b^{+} myeloid-derived suppressor cells (green) and CD31 (red) in non-small cell lung cancer xenografts. Blue fluorescence indicates DAPI (nuclear) staining. (A) The F0 (control) group possessed a large percentage of CD11b^{+} cells. (B) F1, (C) F2 and (D) F3 groups exhibited a lower percentage of CD11b^{+} compared with that in F0. (E) The percentage of CD11b^{+} cells in the F4 group was similar to that in F0 and higher compared with that in F1, F2 and F3. CD, cluster of differentiation; F0 mice, injected with A549 cells only; F1 mice, injected with A549 cells and treated with B20 twice weekly; F2 mice, transplanted with F1 tumor explant and treated with B20 twice weekly; F3 mice, transplanted with F2 tumor explant and treated with B20 twice weekly; F4 mice, transplanted with F3 tumor explant with no treatment.

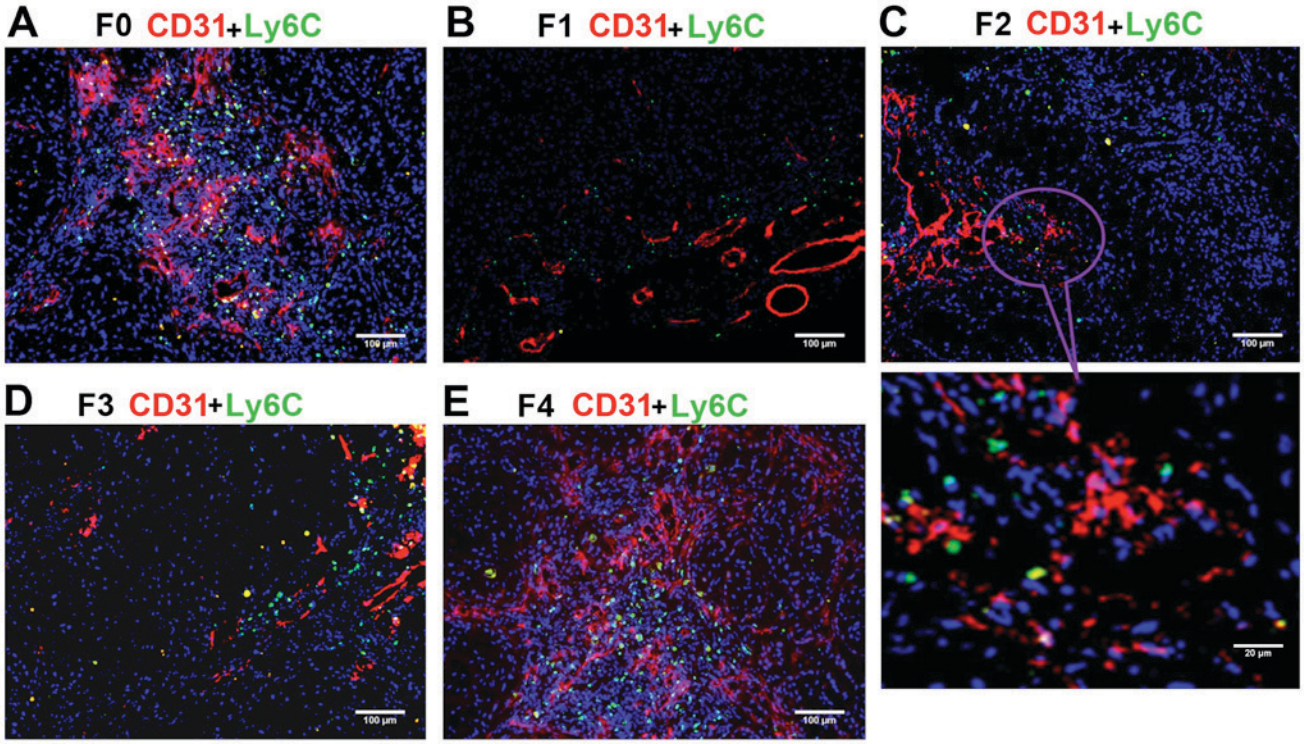

Figure 4. Immunostaining of Ly6C$^+$ cell subsets (green) and CD31 (red) in non-small cell lung cancer xenografts. Blue fluorescence indicates DAPI (nuclear) staining. (A) The F0 (control) group had a large percentage of Ly6C$^+$ cells. (B) F1, (C) F2 and (D) F3 groups displayed a lower percentage of Ly6C$^+$ compared with that in F0. (E) The percentage of Ly6C$^+$ in the F4 group was similar to that in F0 and higher compared with that in F1, F2 and F3. Ly6C, lymphocyte antigen 6C; CD, cluster of differentiation; F0 mice, injected with A549 cells only; F1 mice, injected with A549 cells and treated with B20 twice weekly; F2 mice, transplanted with F1 tumor explant and treated with B20 twice weekly; F3 mice, transplanted with F2 tumor explant and treated with B20 twice weekly; F4 mice, transplanted with F3 tumor explant with no treatment.

was significantly lower in each of these three B20-treated groups compared with in the F0 and F4 groups (all P<0.01; Table I). The changes observed in the number of CD11b$^+$ cells were consistent with those of CD31$^+$ endothelial cells. These results indicated that anti-VEGF antibody effectively decreased the recruitment of MDSCs to the tumor tissue, thus inhibiting the vessel formation in F1, F2, and F3 groups. The lower presence of CD11b$^+$ myeloid cells in the F3 compared with the F0 group demonstrated that drug resistance was not successfully induced.

Assessment of Ly6C$^+$ subset of CD11b$^+$ MDSCs. The anti-Ly6C antibody was used to mark the Ly6C$^+$ subset of CD11b$^+$ MDSCs, which may serve an essential role in promoting angiogenesis and tumor progression. The ratio of Ly6C$^+$ cells (green) to all cells in the field of vision (blue) was calculated. The blood vessels were simultaneously marked by staining of CD31. Under a confocal microscope, the largest numbers of Ly6C$^+$ monocytes were present in the F0 (control) and F4 groups (Fig. 4), and the number of Ly6C$^+$ monocytes decreased from F1 (Fig. 4B) to F2 (Fig. 4C) to F3 (Fig. 4D), indicating inhibitory effects of the anti-VEGF antibody on Ly6C$^+$ monocyte migration and angiogenesis. Consistent with the trend for CD11b$^+$ cells, the percentage of Ly6C$^+$ monocytes in the field of vision (Ly6C ratio) continuously decreased from the F1 to F2 to F3 groups, and was significantly lower in each of these three groups compared with in the F0 and F4 groups (P<0.01; Table II). These data indicated that anti-VEGF antibody repressed the migration of MDSCs, including the Ly6C$^+$ subpopulation, to the tumor tissue, and that drug resistance had not been acquired. To further determine the migration tendency of Ly6C$^+$CD11b$^+$ monocytes, the ratio of Ly6C$^+$ monocytes to CD11b$^+$ MDSCs (Ly6C/CD11b) was calculated. Notably, it was identified that the Ly6C/CD11b ratio was highest in the F3 group and significantly higher in F3 compared with in F0, F1, and F4 groups (all P<0.01) (Table II). These findings suggested that the migration tendency of the Ly6C$^+$ subset relatively increased with the increasing mouse generation compared with

Table II. Ly6C and Ly6C/CD11b ratios in non-small cell lung cancer xenografts.

Group	CD31 ratio	Ly6C ratio	Ly6C/CD11^b
F0	0.18±0.03^a	0.06±0.01^a	0.38±0.05
F1	0.10±0.02	0.05±0.01	0.44±0.10
F2	0.06±0.02	0.04±0.01	0.51±0.13
F3	0.04±0.01	0.04±0.00	0.68±0.11^b
F4	0.17±0.02^a	0.06±0.01^a	0.40±0.10

^{a}P<0.01 vs. F1, F2 and F3 groups; ^{b}P<0.01 vs. F0, F1 and F4 groups. CD, cluster of differentiation; Ly6, lymphocyte antigen 6C; F0, mice injected with A549 cells only; F1, mice injected with A549 cells and treated with B20 twice weekly; F2, mice transplanted with F1 tumor explant and treated with B20 twice weekly; F3, mice transplanted with F2 tumor explant and treated with B20 twice weekly; F4, mice transplanted with F3 tumor explant with no treatment.

the other subsets in the whole CD11b$^+$ population. Thus, if the generations of nude mice or the tumor growth period (between inoculation and harvesting) is increased, it is possible that the xenograft model of acquired resistance to anti-VEGF antibody may be successfully established.

Discussion

Molecular inhibition of VEGF/VEGFR signaling is currently being investigated as a promising cancer treatment strategy. For lung cancer, one study has demonstrated that angiogenesis inhibitors are superior to non-angiogenesis inhibitors with regard to objective response, disease control, progression-free survival and overall survival rates in patients with advanced NSCLC (18). The advantages of anti-angiogenesis therapy have mostly been demonstrated with antibody-based agents (48). Monoclonal antibodies against VEGF, such as bevacizumab, have demonstrated efficacy when used alone or in combination with chemotherapy (49). However, modest effects have been reported and drug resistance has been widely observed in preclinical and clinical trials (17,50,51). Thus, efforts to better understand the mechanisms underlying acquired resistance to anti-VEGF antibodies and potential strategies to overcome resistance are warranted.

In the present study, the aim was to establish an NSCLC xenograft model of acquired resistance to anti-VEGF antibody in nude mice, in order to provide a tool for mechanism investigation and future research, and then to detect the expression of CD31 and the migration of CD11b$^+$Ly6C$^+$ monocytes. In the xenotransplantation experiments, tumor growth rate in the last generation of drug administration (F3) was lower compared with that in the control (F0). Following immunostaining, the expression of CD31 was revealed to be lower in the F3 group compared with that in the F0 group. These data indicated that the drug resistance model had not been successfully established.

It was hypothesized that these negative data may result from the changing microenvironment in distinct generations of mice. It has been recognized that the development of resistance to anti-angiogenesis agents is largely associated with the tumor microenvironment, including stromal cells, extracellular matrix-components, TAMs, and autocrine and paracrine signaling factors (52). Tumor cells communicate with components of their microenvironment via a complex network of growth factors, cytokines and chemokines. TAMs support lung cancer progression by inducing cancer cell motility and metastasis, and angiogenesis (52,53). As a result, changing the microenvironment of the tumor leads to updated recruitment of accessory cells and molecules, thus decreasing the tumor growth rate in xenografts. Therefore, elongation of the period between tumor inoculation and harvesting may compensate for the change in microenvironment. In the present study, the mice were sacrificed on day 29 post-inoculation in F1 group, on day 21 in F2 group, day 25 in F3 group, and day 25 in F4 group. However, in a similar study, Gyanchandani *et al* (54) generated a head and neck squamous cell carcinoma xenograft model of acquired resistance to bevacizumab, in which the time for a generation was ≥56 days. In the study by Curtarello *et al* (55), mice were maintained for ≥45 days after tumor inoculation to induce resistance to bevacizumab in ovarian and breast cancer cells. In the present study, the Ly6C/CD11b ratio increased from the F1 to the F3 group. A larger number of generations may promote the successful acquisition of resistance to anti-VEGF antibody by tumor cells. The short time and low generation numbers of the present study were its limitations.

However, the ratio of Ly6C/CD11b was higher in the F3 group compared with that in the other groups, suggesting an enhanced migration tendency of the Ly6C$^+$ subset. This subset is a population of cells that are able to polarize into M2 macrophages and serve a role in promoting angiogenesis (38,39). The primary functions of M2 macrophages are limitation of the immune response and promotion of tumor invasion, growth and metastasis via the secretion of inhibitory cytokines and the prevention of T cells from exerting antitumor effects (56). Although Ly6C$^+$ and Ly6G$^+$ MDSC numbers are equally increased in tumor-bearing mice (36), the Ly6C$^+$ subset has a greater tendency to polarize into M2 macrophages following proper stimulation. In contrast to these reports, Ly6C^{hi} monocytes are preferentially recruited to inflamed tissues in a C-C motif chemokine receptor-2-dependent manner and generate inflammatory macrophages, such as M1 macrophages, as described in myocardial infarction (57), muscle injury (58), and bacterial infection (59). Ly6C^{hi} monocytes digest damaged tissue, whereas Ly6C^{lo} monocytes promote healing via myofibroblast accumulation, angiogenesis and deposition of collagen (57). It appears that Ly6C^{hi} monocytes cooperate with M1 macrophages in inflammatory functions, whereas Ly6C^{lo} monocytes work together with M2 macrophages to achieve angiogenic functions (60). Notably, Ly6C^{hi} monocytes can give rise to Ly6C^{lo} monocytes under steady-state conditions (61-63). Therefore, regardless of whether M2 macrophages derive from Ly6C^{hi} or Ly6C^{lo} monocytes, increased recruitment of Ly6C^{hi} monocytes indicates enhanced angiogenesis.

Although Shojaei *et al* (30) did not provide definitive evidence of macrophage involvement in tumor refractoriness following anti-VEGF therapy, it was revealed that tumor relapse is affected by the heterogeneous CD11b$^+$Gr-1$^+$ MDSCs; the combination of anti-VEGF and anti-Gr-1 antibodies given to tumor-bearing mice was more effective in preventing angiogenesis and slowing tumor growth compared with either antibody alone. Since the Gr-1 antibody recognizes Ly6C, a receptor expressed on inflammatory monocytes, and Ly6G, it can be inferred that monocytes/macrophages may be partially responsible for refractoriness following anti-angiogenic therapy. Notably, resistance to conventional chemotherapies did not involve CD11b$^+$Gr-1$^+$ MDSCs in these models, suggesting that myeloid cells specifically initiate refractoriness to anti-angiogenic therapies (30).

Other studies have demonstrated upregulation of VEGF expression in macrophages following radiotherapy in patients, suggesting that increased levels of TAM-derived pro-angiogenic factors can stimulate the formation of a new blood supply to radio-resistant tumor cells (64). In agreement with these data, Ahn *et al* (65) revealed the important contribution of matrix metallopeptidase 9-expressing CD11b$^+$ myeloid cells to tumor revascularization and recovery following radiation. Taken together, these findings indicate that inhibiting monocyte recruitment to tumors or neutralizing the factors that they produce in tumors, in combination with conventional therapeutic agents, may have considerable therapeutic potential.

In conclusion, in the current study, the increased migration tendency of $CD11b^{+}Ly6C^{+}$ myeloid cells suggests the potential for successful resistance acquisition and implies a possible contribution of these cells to tumor refractoriness. Increasing the number of generations or the time for post-inoculation tumor growth may generate an NSCLC model of acquired resistance to the anti-VEGF antibody. The role of $CD11b^{+}Ly6C^{+}$ monocytes in angiogenesis and their association with M2 macrophages may have implications for improving the efficacy of anti-VEGF therapies.

Acknowledgements

The present study was supported by the National Science Foundation of China (grant nos. 30772108 and 81272910) and the Chongqing Natural Science Foundation (grant no. cstc2012jjA10096). The authors would like to thank Drs J. Martin Brown and Sophia (School of Medicine, Stanford University, Stanford, CA, USA) for their instructions, and Mr. Dian-Gang Chen (Cancer Institute of People's Liberation Army, Xinqiao Hospital, Third Military Medical University, Chongqing, China) for guidance on experimental techniques.

References

1. Allemani C, Weir HK, Carreira H, Harewood R, Spika D, Wang XS, Bannon F, Ahn JV, Johnson CJ, Bonaventure A, *et al*: Global surveillance of cancer survival 1995-2009: Analysis of individual data for 25,676,887 patients from 279 population-based registries in 67 countries (CONCORD-2). Lancet 385: 977-1010, 2015.
2. Torre LA, Bray F, Siegel RL, Ferlay J, Lortet-Tieulent J and Jemal A: Global cancer statistics, 2012. CA Cancer J Clin 65: 87-108, 2015.
3. Stinchcombe TE and Socinski MA: Current treatments for advanced stage non-small cell lung cancer. Proc Am Thorac Soc 6: 233-241, 2009.
4. Morgensztern D, Waqar S, Subramanian J, Gao F and Govindan R: Improving survival for stage IV non-small cell lung cancer: A surveillance, epidemiology, and end results survey from 1990 to 2005. J Thorac Oncol 4: 1524-1529, 2009.
5. Zetter BR: Angiogenesis and tumor metastasis. Annu Rev Med 49: 407-424, 1998.
6. Carmeliet P: Angiogenesis in life, disease and medicine. Nature 438: 932-936, 2005.
7. Weidner N: Intratumor microvessel density as a prognostic factor in cancer. Am J Pathol 147: 9-19, 1995.
8. Dvorak HF, Sioussat TM, Brown LF, Berse B, Nagy JA, Sotrel A, Manseau EJ, Van de Water L and Senger DR: Distribution of vascular permeability factor (vascular endothelial growth factor) in tumors: Concentration in tumor blood vessels. J Exp Med 174: 1275-1278, 1991.
9. Kim KJ, Li B, Winer J, Armanini M, Gillett N, Phillips HS and Ferrara N: Inhibition of vascular endothelial growth factor-induced angiogenesis suppresses tumour growth in vivo. Nature 362: 841-844, 1993.
10. Toi M, Matsumoto T and Bando H: Vascular endothelial growth factor: Its prognostic, predictive, and therapeutic implications. Lancet Oncol 2: 667-673, 2001.
11. Ferrara N: Vascular endothelial growth factor as a target for anticancer therapy. Oncologist 9 (Suppl 1): S2-S10, 2004.
12. Hu P, Liu W, Wang L, Yang M and Du J: High circulating VEGF level predicts poor overall survival in lung cancer. J Cancer Res Clin Oncol 139: 1157-1167, 2013.
13. Chen P, Zhu J, Liu DY, Li HY, Xu N and Hou M: Over-expression of survivin and VEGF in small-cell lung cancer may predict the poorer prognosis. Med Oncol 31: 775, 2014.
14. Chen J, Tang D, Wang S, Li QG, Zhang JR, Li P, Lu Q, Niu G, Gao J, Ye NY and Wang DR: High expressions of galectin-1 and VEGF are associated with poor prognosis in gastric cancer patients. Tumor Biol 35: 2513-2519, 2014.
15. Folkman J: Tumor angiogenesis: Therapeutic implications. N Engl J Med 285: 1182-1186, 1971.
16. Piperdi B, Merla A and Perez-Soler R: Targeting angiogenesis in squamous non-small cell lung cancer. Drugs 74: 403-413, 2014.
17. Pallis AG and Syrigos KN: Targeting tumor neovasculature in non-small-cell lung cancer. Crit Rev Oncol Hematol 86: 130-142, 2013.
18. Zhou C, Wu YL, Chen G, Liu X, Zhu Y, Lu S, Feng J, He J, Han B, Wang J, *et al*: BEYOND: A randomized, double-blind, placebo-controlled, multicenter, phase III study of first-line carboplatin/paclitaxel plus bevacizumab or placebo in Chinese patients with advanced or recurrent nonsquamous non-small-cell lung cancer. J Clin Oncol 33: 2197-2204, 2015.
19. Tejpar S, Prenen H and Mazzone M: Overcoming resistance to antiangiogenic therapies. Oncologist 17: 1039-1050, 2012.
20. Sica A and Bronte V: Altered macrophage differentiation and immune dysfunction in tumor development. J Clin Invest 117: 1155-1166, 2007.
21. Kusmartsev S and Gabrilovich DI: Role of immature myeloid cells in mechanisms of immune evasion in cancer. Cancer Immunol Immunother 55: 237-245, 2006.
22. Rabinovich GA, Gabrilovich D and Sotomayor EM: Immunosuppressive strategies that are mediated by tumor cells. Annu Rev Immunol 25: 267-296, 2007.
23. Talmadge JE: Pathways mediating the expansion and immunosuppressive activity of myeloid-derived suppressor cells and their relevance to cancer therapy. Clin Cancer Res 13: 5243-5248, 2007.
24. Almand B, Clark JI, Nikitina E, van Beynen J, English NR, Knight SC, Carbone DP and Gabrilovich DI: Increased production of immature myeloid cells in cancer patients: A mechanism of immunosuppression in cancer. J Immunol 166: 678-689, 2001.
25. Young MR and Lathers DM: Myeloid progenitor cells mediate immune suppression in patients with head and neck cancers. Int J Immunopharmacol 21: 241-252, 1999.
26. Ebos JM, Lee CR and Kerbel RS: Tumor and host-mediated pathways of resistance and disease progression in response to antiangiogenic therapy. Clin Cancer Res 15: 5020-5025, 2009.
27. Kioi M, Vogel H, Schultz G, Hoffman RM, Harsh GR and Brown JM: Inhibition of vasculogenesis, but not angiogenesis, prevents the recurrence of glioblastoma after irradiation in mice. J Clin Invest 120: 694-705, 2010.
28. Yang L, Huang J, Ren X, Gorska AE, Chytil A, Aakre M, Carbone DP, Matrisian LM, Richmond A, Lin PC and Moses HL: Abrogation of TGF beta signaling in mammary carcinomas recruits $Gr\text{-}1^{+}CD11b^{+}$ myeloid cells that promote metastasis. Cancer Cell 13: 23-35, 2008.
29. Chan DA, Kawahara TL, Sutphin PD, Chang HY, Chi JT and Giaccia AJ: Tumor vasculature is regulated by PHD2-mediated angiogenesis and bone marrow-derived cell recruitment. Cancer Cell 15: 527-538, 2009.
30. Shojaei F, Wu X, Malik AK, Zhong C, Baldwin ME, Schanz S, Fuh G, Gerber HP and Ferrara N: Tumor refractoriness to anti-VEGF treatment is mediated by $CD11b^{+}Gr1^{+}$ myeloid cells. Nat Biotechnol 25: 911-920, 2007.
31. Yang L, DeBusk LM, Fukuda K, Fingleton B, Green-Jarvis B, Shyr Y, Matrisian LM, Carbone DP and Lin PC: Expansion of myeloid immune suppressor $Gr^{+}CD11b^{+}$ cells in tumor-bearing host directly promotes tumor angiogenesis. Cancer Cell 6: 409-421, 2004.
32. Shojaei F, Wu X, Zhong C, Yu L, Liang XH, Yao J, Blanchard D, Bais C, Peale FV, van Bruggen N, *et al*: Bv8 regulates myeloid-cell-dependent tumour angiogenesis. Nature 450: 825-831, 2007.
33. Youn JI, Nagaraj S, Collazo M and Gabrilovich DI: Subsets of myeloid-derived suppressor cells in tumor-bearing mice. J Immunol 181: 5791-5802, 2008.
34. Sawanobori Y, Ueha S, Kurachi M, Shimaoka T, Talmadge JE, Abe J, Shono Y, Kitabatake M, Kakimi K, Mukaida N and Matsushima K: Chemokine-mediated rapid turnover of myeloid-derived suppressor cells in tumor-bearing mice. Blood 111: 5457-5466, 2008.
35. Dietlin TA, Hofman FM, Lund BT, Gilmore W, Stohlman SA and van der Veen RC: Mycobacteria-induced Gr-1+ subsets from distinct myeloid lineages have opposite effects on T cell expansion. J Leukoc Biol 81: 1205-1212, 2007.
36. Movahedi K, Guilliams M, Van den Bossche J, Van den Bergh R, Gysemans C, Beschin A, De Baetselier P and Van Ginderachter JA: Identification of discrete tumor-induced myeloid-derived suppressor cell subpopulations with distinct T cell-suppressive activity. Blood 111: 4233-4244, 2008.

37. Avraham-Davidi I, Yona S, Grunewald M, Landsman L, Cochain C, Silvestre JS, Mizrahi H, Faroja M, Strauss-Ayali D, Mack M, *et al*: On-site education of VEGF-recruited monocytes improves their performance as angiogenic and arteriogenic accessory cells. J Exp Med 210: 2611-2625, 2013.
38. Gordon S: Alternative activation of macrophages. Nat Rev Immunol 3: 23-35, 2003.
39. Gordon S and Taylor PR: Monocyte and macrophage heterogeneity. Nat Rev Immunol 5: 953-964, 2005.
40. Murdoch C, Muthana M, Coffelt SB and Lewis CE: The role of myeloid cells in the promotion of tumour angiogenesis. Nat Rev Cancer 8: 618-631, 2008.
41. Mantovani A, Allavena P, Sica A and Balkwill F: Cancer-related inflammation. Nature 454: 436-444, 2008.
42. Comito G, Giannoni E, Segura CP, Barcellos-de-Souza P, Raspollini MR, Baroni G, Lanciotti M, Serni S and Chiarugi P: Cancer-associated fibroblasts and M2-polarized macrophages synergize during prostate carcinoma progression. Oncogene 33: 2423-2431, 2014.
43. Denney L, Kok WL, Cole SL, Sanderson S, McMichael AJ and Ho LP: Activation of invariant NKT cells in early phase of experimental autoimmune encephalomyelitis results in differentiation of Ly6Chi inflammatory monocyte to M2 macrophages and improved outcome. J Immunol 189: 551-557, 2012.
44. Chu HX, Broughton BR, Kim HA, Lee S, Drummond GR and Sobey CG: Evidence that Ly6C(hi) monocytes are protective in acute ischemic stroke by promoting M2 macrophage polarization. Stroke 46: 1929-1937, 2015.
45. Jalali S, Chung C, Foltz W, Burrell K, Singh S, Hill R and Zadeh G: MRI biomarkers identify the differential response of glioblastoma multiforme to anti-angiogenic therapy. Neuro Oncol 16: 868-879, 2014.
46. Naito S, von Eschenbach AC, Giavazzi R and Fidler IJ: Growth and metastasis of tumor cells isolated from a human renal cell carcinoma implanted into different organs of nude mice. Cancer Res 46: 4109-4115, 1986.
47. Ahn GO, Tseng D, Liao CH, Dorie MJ, Czechowicz A and Brown JM: Inhibition of Mac-1 (CD11b/CD18) enhances tumor response to radiation by reducing myeloid cell recruitment. Proc Natl Acad Sci USA 107: 8363-8368, 2010.
48. Hong S, Tan M, Wang S, Luo S, Chen Y and Zhang L: Efficacy and safety of angiogenesis inhibitors in advanced non-small cell lung cancer: A systematic review and meta-analysis. J Cancer Res Clin Oncol 141: 909-921, 2015.
49. Blakely C and Jahan T: Emerging antiangiogenic therapies for non-small-cell lung cancer. Expert Rev Anticancer Ther 11: 1607-1618, 2011.
50. Giuliano S and Pagès G: Mechanisms of resistance to anti-angiogenesis therapies. Biochimie 95: 1110-1119, 2013.
51. Sitohy B, Nagy JA and Dvorak HF: Anti-VEGF/VEGFR therapy for cancer: Reassessing the target. Cancer Res 72: 1909-1914, 2012.
52. Wood SL, Pernemalm M, Crosbie PA and Whetton AD: The role of the tumor-microenvironment in lung cancer-metastasis and its relationship to potential therapeutic targets. Cancer Treat Rev 40: 558-566, 2014.
53. Saintigny P and Burger JA: Recent advances in non-small cell lung cancer biology and clinical management. Discov Med 13: 287-297, 2012.
54. Gyanchandani R, Ortega Alves MV, Myers JN and Kim S: A proangiogenic signature is revealed in FGF-mediated bevacizumab-resistant head and neck squamous cell carcinoma. Mol Cancer Res 11: 1585-1596, 2013.
55. Curtarello M, Zulato E, Nardo G, Valtorta S, Guzzo G, Rossi E, Esposito G, Msaki A, Pastò A, Rasola A, *et al*: VEGF-targeted therapy stably modulates the glycolytic phenotype of tumor cells. Cancer Res 75: 120-133, 2015.
56. Mira E, Carmona-Rodríguez L, Tardáguila M, Azcoitia I, González-Martín A, Almonacid L, Casas J, Fabriás G and Mañes S: A lovastatin-elicited genetic program inhibits M2 macrophage polarization and enhances T cell infiltration into spontaneous mouse mammary tumors. Oncotarget 4: 2288-2301, 2013.
57. Nahrendorf M, Swirski FK, Aikawa E, Stangenberg L, Wurdinger T, Figueiredo JL, Libby P, Weissleder R and Pittet MJ: The healing myocardium sequentially mobilizes two monocyte subsets with divergent and complementary functions. J Exp Med 204: 3037-3047, 2007.
58. Arnold L, Henry A, Poron F, Baba-Amer Y, van Rooijen N, Plonquet A, Gherardi RK and Chazaud B: Inflammatory monocytes recruited after skeletal muscle injury switch into antiinflammatory macrophages to support myogenesis. J Exp Med 204: 1057-1069, 2007.
59. Auffray C, Fogg D, Garfa M, Elain G, Join-Lambert O, Kayal S, Sarnacki S, Cumano A, Lauvau G and Geissmann F: Monitoring of blood vessels and tissues by a population of monocytes with patrolling behavior. Science 317: 666-670, 2007.
60. Anzai A, Anzai T, Nagai S, Maekawa Y, Naito K, Kaneko H, Sugano Y, Takahashi T, Abe H, Mochizuki S, *et al*: Regulatory role of dendritic cells in postinfarction healing and left ventricular remodeling. Circulation 125: 1234-1245, 2012.
61. Varol C, Landsman L, Fogg DK, Greenshtein L, Gildor B, Margalit R, Kalchenko V, Geissmann F and Jung S: Monocytes give rise to mucosal, but not splenic, conventional dendritic cells. J Exp Med 204: 171-180, 2007.
62. Ancuta P, Liu KY, Misra V, Wacleche VS, Gosselin A, Zhou X and Gabuzda D: Transcriptional profiling reveals developmental relationship and distinct biological functions of CD16+ and CD16- monocyte subsets. BMC Genomics 10: 403, 2009.
63. Hettinger J, Richards DM, Hansson J, Barra MM, Joschko AC, Krijgsveld J and Feuerer M: Origin of monocytes and macrophages in a committed progenitor. Nat Immunol 14: 821-830, 2013.
64. McDonnell CO, Bouchier-Hayes DJ, Toomey D, Foley D, Kay EW, Leen E and Walsh TN: Effect of neoadjuvant chemoradiotherapy on angiogenesis in oesophageal cancer. Br J Surg 90: 1373-1378, 2003.
65. Ahn GO and Brown JM: Matrix metalloproteinase-9 is required for tumor vasculogenesis but not for angiogenesis: Role of bone marrow-derived myelomonocytic cells. Cancer Cell 13: 193-205, 2008.